XBP1s Activation Can Globally Remodel *N*-Glycan Structure Distribution Patterns

Madeline Y. Wong, Kenny Chen, Aristotelis Antonopoulos, Brian T. Kasper, Mahender B. Dewal, Rebecca J. Taylor, Charles A. Whittaker, Pyae P. Hein, Anne Dell, Joseph C. Genereux, Stuart M. Haslam, Lara K. Mahal, and Matthew D. Shoulders

www.pnas.org/cgi/doi/10.1073/pnas.1805425115

SUPPORTING EXPERIMENTAL PROCEDURES

Cells and Reagents. HEK^{XBP1s} cells were cultured as previously described (1). HeLa-TREx cells were obtained from Invitrogen and cultured in complete DMEM supplemented with 10% fetal bovine serum (FBS), as well as geneticin sulfate (G418, 500 μg/mL) to maintain the tetracycline repressor. A pLenti4.XBP1s construct, along with a linear marker for puromycin resistance, was transfected into HeLa.TREx cells using Xfect (Clontech). Stable HeLa^{XBP1s} cell lines were selected by culturing in puromycin (0.5 μg/mL). An optimized single colony was selected and characterized by Western blot and qPCR before use in these experiments.

Lectin Microarray Glycomic Analyses. Lectin microarrays were generated as previously described (2). Briefly, they were manufactured in-house with a Nano-plotter v2.0 piezoelectric non-contact array printer (GeSiM) using a nano A-J tip. Arrays were printed on Nexterion Slide H (Schott Nexterion) under 50% relative humidity at a surface temperature of 12 °C. Commercial lectins and antibodies were purchased from Vector Labs, R&D Systems, Santa Cruz, TCI, AbCam, E.Y. Labs, or Sigma-Aldrich. The recombinant lectins rGRFT, rCVN, and rSVN were generous gifts from Dr. B. O'Keefe (NCI Frederick). For a list of all printed lectins see Dataset S2. We note that while the diversity of printed lectins allows for a wide range in the detection of glycan epitopes, we are unable to observe some epitopes (e.g. α2,8-linked sialic acids) on our current array.

Prior to sample hybridization, lectin microarray slides were blocked for 1 h with 50 mM ethanolamine in 50 mM sodium borate buffer (pH 8.8) followed by three washes with 0.005% PBS-T (pH 7.4). Sample protein concentration and the degree of fluorescent label incorporation was determined by measuring absorbances at 280, 555, and 650 nm per the manufacturer's instructions on a NanoDrop ND-2000c spectrophotometer (Thermo Scientific). Equal protein amounts (5 μg) of sample and contrasting labeled reference were mixed in 0.005% PBS-T (pH 7.4) for a final concentration of 67 ng/μL of protein. Slides were then loaded into a hybridization cassette (Arrayit) to isolate individual arrays (24 per slide). Samples were loaded onto individual arrays along with one array for the reference vs reference sample per slide. Samples were hybridized for 2 h at 25 °C with gentle agitation. After hybridization, samples were removed and arrays were washed 4× with 0.005% PBS-T (pH 7.4) for 10 min each. Slides were removed, submerged in ddH_2O, and spun dry. Arrays were scanned using a GenePix 4300A array scanner (PMT 550 laser power 100% for both fluorescent channels).

Background-subtracted median fluorescence intensities were extracted using GenePix Pro v7.2. Non-active lectins were defined as having an average of both channel SNRs <3 in >90% of the data and removed prior to further analysis. Data were median-normalized in each fluorescent channel and the log2 of the sample/reference ratio was calculated for each technical replicate for each lectin. Technical replicates were then averaged for each lectin within each array. The ratios across individual biological triplicates per lectin were compared across treatments using a two-tailed Student's *t*-test.

MALDI-TOF MS and TOF/TOF MS/MS Glycomic Analyses. All samples were treated as described previously (3). Briefly, each sample was subjected to sonication in the presence of detergent (CHAPS), reduction in 4 M guanidine-HCl (Pierce, Cramlington, Northumberland, UK), carboxymethylation, and trypsin digestion. The digested glycoproteins were then purified by HLB plus C_{18}-Sep-Pak (Waters Corp, Hertfordshire, UK; 186000132). *N*-Glycans were released by peptide *N*-glycosidase F (E.C. 3.5.1.52; Roche Applied Science, Burgess Hill, UK) digestion. Released *N*-glycans were permethylated using the sodium hydroxide procedure and purified by classic C_{18}-Sep-Pak (Waters, WAT051910). Permethylated *N*-glycans were eluted at the 50% acetonitrile fraction. We note that polysialylated structures deriving from the activity of α2,8-sialyltransferase (ST8SIA2) enzyme were not analyzed from the above released *N*-glycans (4).

MS and MS/MS data were acquired using a 4800 MALDI-TOF/TOF (Applied Biosystems, Darmstadt, Germany) mass spectrometer. Permethylated samples were dissolved in 10 μL of methanol and 1 μL of dissolved sample was premixed with 1 μL of matrix (10 mg/mL 3,4-diaminobenzophenone in 75% (v/v) aqueous acetonitrile), spotted onto a target plate and dried under vacuum. For the MS/MS studies the collision energy was set to 1 kV, and Ar was used as the collision gas. The 4700 Calibration standard kit, calmix (Applied Biosystems), was used as the external calibrant for the MS mode and [Glu1] fibrinopeptide B human (Sigma-Aldrich) was used as an external calibrant for the MS/MS mode.

MS and MS/MS data were processed using Data Explorer 4.9 Software (Applied Biosystems). The processed spectra were subjected to manual assignment and annotation with the aid of a glycobioinformatics tool, GlycoWorkBench (5). The proposed assignments for the selected peaks were based on ^{12}C isotopic composition together with knowledge of the biosynthetic pathways. The proposed structures were then confirmed by data obtained from MS/MS and linkage analysis experiments.

For MALDI-TOF analysis of secretome samples, we note that even in commercial "serum-free" media, MS detects serum-derived glycoproteins (6). In prior work we have shown that the FBS-derived glycans can be identified and removed from the analysis without impacting analysis of other glycan structures, just as we have done here (7, 8). Thus, the presence of these peaks does not significantly impact detection of other glycan structures in the secretome.

GC-MS Glycan Linkage Analyses. Partially methylated alditol acetates (PMAAs) were prepared as previously described (3). Linkage analyses of PMAAs were performed on a Scion 456-GC SQ instrument (Bruker) fitted with a BR-5ms fused silica capillary column (15 m × 0.25 mm i.d.; Bruker). The sample was dissolved in ~20 μL of hexanes and injected manually (4–5 μL) at a split ratio of 1/10. Injector temperature was set at 250 °C. Helium was used a carrier gas at constant flow of 1 mL/min. PMAAs were eluted with the following linear gradient oven: initially the oven temperature was set at 60 °C for 1 min, heated to 300 °C at a rate of 8 °C per min, then held at 300 °C for 1 min.

RNA Extraction and Real-Time qPCR. HEK^{XBP1s} and HeLa^{XBP1s} cells were plated and treated as for lectin microarray analysis (below). After 72 h of XBP1s activation with 1 μg/mL dox (or 24 h of treatment with 0.1% DMSO or 750 nM Tg), cells were washed with PBS and RNA was extracted using the Omega E.Z.N.A. Total RNA extraction kit. cDNA was prepared from 500 ng RNA, normalized for all samples in each run, using an Applied Biosystems Reverse Transcriptase cDNA Kit in a BioRad Thermocycler. Samples were run on a Light Cycler 480 II Real Time PCR Instrument in the MIT BioMicro Center using previously described primers and data were analyzed as described previously (1, 9). For qPCR arrays, HEK^{XBP1s} and HeLa^{XBP1s} cells were treated for 48 h with 1 μg/mL dox or 0.1% DMSO prior to harvesting. RNA was then extracted using the Qiagen RNeasy kit, cDNA was prepared from equal amounts of RNA using the Qiagen RT2 First Strand Kit in a Bio-Rad Thermocycler, and samples were loaded on an RT^2 Profiler PCR Array for Human Glycosylation (Qiagen PAHS-046Z). Analyses were performed in a Light Cycler 480 II Real Time PCR Instrument in the MIT BioMicro Center. Data from three biological replicates were analyzed using the ΔΔCt method. A list of glycogenes was manually curated from the HEK^{XBP1s} microarray (9) and HeLa^{XBP1s} RNA-Seq data, and then combined with detected glycogenes from the PCR array (Dataset S5). Significance cut-offs used were FDR or *p*-value ≤ 0.05 and fold-change ≥ 1.5.

RNA-Seq. HeLa^{XBP1s} cells were plated in biological triplicate at a density of 6 × 10^5 cells per well in 6-well plates and allowed to adhere overnight. Cells were then treated for 48 h with vehicle or 1 μg/mL dox, or for 24 h with 750 nM Tg. Cells were harvested and RNA was extracted using the RNeasy Plus Mini Kit (Qiagen). RNA quality was confirmed using a Fragment Analyzer (Advanced Analytical). RNA samples were then loaded on a HiSeq cartridge as a 50 base single-end run with 6 + 6 nucleotide indexes. *H. sapiens* RNA-Seq reads were aligned to hg19 with bowtie version 1.0.1 (10) and expression was summarized using rsem version 1.2.26 (11) using the ensemble gencode annotation release 75. Differential expression analysis was done with deseq2 version 1.10.0 (12) running under R version 3.2.3. Default options were selected for deseq2 runs, except Cooks Cutoff and Independent Filtering were both set to false during results preparation. Gene Set Enrichment Analysis (13) Java command-line version 2.3.0 beta was run in both pre-ranked and standard mode using the stat output from deseq2 to order genes. Custom gene sets and a selected subset from MSigDB version 5.2 were analyzed; these gene sets are provided in Datasets S1E and S5A. Hierarchical clustering was performed with Spotfire 7.6.1, using counts of transcripts with highest expression for each gene.

Membrane Proteome Preparation. HeLa^{XBP1s} or HEK293^{XBP1s} cells were plated in 10 cm dishes at a density of 1 × 10^6 cells per plate and allowed to adhere overnight. The next day, XBP1s expression was induced by treatment with 1 μg/mL dox. Vehicle and Tg-treated plates received fresh media and either DMSO or 750 nM

Tg for 24 h before harvesting. After 72 h of induction, cells were harvested by scraping in 1× PBS + 1 mM EDTA, sonicated to disrupt cells, and then centrifuged at 35k RPM at 4 °C for 1 h to pellet the membrane fraction. Pellets were resuspended in 100 μL PBS, homogenized with 21G and 27G needles, and protein concentrations were measured via A280 on a NanoDrop ND-1000 spectrophotometer.

Secretome Preparation from HEK^{XBP1s} Cells. Prior to plating cells, 15 cm dishes were coated with 0.05 mg/mL of poly-D-lysine hydrobromide (Sigma P6407) for 10 min at room temperature. Each dish was washed three times with PBS before seeding with 10 × 10^6 HEK^{XBP1s} cells in complete medium. After 24 h, media were changed to add the appropriate compounds: 1 μg/mL dox for XBP1s activation or 0.1% DMSO for control. After another 24 h, media were removed and cells were washed with PBS (containing Ca^{2+} and Mg^{2+}) three times. Cells were then incubated in Freestyle medium (Gibco) with either 1 μg/mL dox, 0.1% DMSO, or 750 nM of Tg. Conditioned media were harvested from cells after a total of 48 h with dox or DMSO, or 28 h with Tg. Medium samples were filtered through 0.2 μm PES membranes (VWR) and concentrated in 3 kDa MWCO centrifugal units (Millipore Amicon Ultra). For immunoblotting analysis of the secretome, 6 × 10^5 HEK^{XBP1s} cells were plated per well on poly-D-lysine coated 6-well plates and treated with dox or vehicle as described above. After 24 h, cells were washed with PBS (containing Ca^{2+} and Mg^{2+}) three times and then incubated in DMEM (+10% FBS, L-glutamine) or Freestyle media, with or without 1 μg/mL dox. Conditioned media were collected after 48 h, spun at 1.5k RPM at 4 °C for 5 min to pellet cell debris, and then run on 4/8% SDS-PAGE gels. Proteins were transferred to nitrocellulose membranes and incubated with an α-KDEL (recognizes both Grp78 and Grp94, Enzo ADI-SPA-827) antibody. Blots were developed with the appropriate 800CW secondary antibody (LI-COR) prior to scanning on an Odyssey infrared imager (LI-COR).

Lectin Flow Cytometry. HeLa^{XBP1s} cells were treated with or without dox for 72 h, then very briefly trypsinized. Cells were washed twice with 2% FBS in PBS, and 1 × 10^6 cells/sample were incubated for 30 min at 4 °C with HHL-biotin (Vector Labs) at 5 μg/mL. Competitive sugars (200 mM α-methylmannoside, Sigma-Aldrich) were pre-incubated 30 min with lectins at room temperature for inhibitory controls. Cells were washed and resuspended in 20 μg/mL of Cy5-streptavidin (Thermo Fisher Scientific) for 20 min at 4 °C in the dark. Cells were resuspended in 1 mL of 2% FBS/PBS, passed through cell strainers (Falcon), and analyzed on a BD Accuri C6 flow cytometer.

CellTiter-Glo Assay. HeLa^{XBP1s} cells were cultured with or without doxycycline (1 μg/mL, 72 h) or 1-DMM (80 μg/mL, 24 h). Cells were counted and plated at 1 × 10^4 cells/well 24 h prior to carrying out the assay according to the manufacturer's instructions (Promega). In brief, cells were cultured in 100 μL of culture media and an equal volume of reagent was added to lyse cells for 2 min. After incubation at room temperature for 10 min, luminescence measurements were taken.

Resazurin Assay. HeLa^{XBP1s} cells were cultured with or without doxycycline (1 μg/mL, 72 h) or 1-DMM (80 μg/mL, 24 h). Cells were counted and plated at 1 × 10^4 cells/well 24 h prior to measurements. Resazurin was added to cells at a final concentration of 0.03 mg/mL for 60 min at 37 °C. Fluorescence readings were taken at 560 nm excitation, 590 nm emission.

Secretome Proteomics Analysis. HEK^{XBP1s} cells were treated with either vehicle or doxycycline for 16 h, washed well, and incubated in DMEM without serum for 6 h. Proteins were then precipitated from conditioned media with 10% TCA for 1.5 h at 4 °C and resolublized using 1% aqueous Rapigest (Waters) in 100 mM HEPES pH 8.0. Proteins were reduced with 5 mM TCEP (Sigma) for 30 min at 37 °C, alkylated with 10 mM iodoacetamide (Sigma) for 30 min in the dark at room temperature, digested with 0.5 μg trypsin overnight at 37 °C and 600 rpm, labeled with appropriate isotopic TMT reagent in 40% CHC_3N for 1 h, quenched with 0.4% ammonium bicarbonate for 1 h, pooled, evaporated, resuspended in buffer A (5% CHC_3N, 0.1% formic acid), brought to pH < 2 with formic acid, heated at 37 °C to precipitate Rapigest, and stored at -80 °C prior to LC/LC-MS/MS analysis.

Nanopure water and mass spectrometry grade solvents were used for all preparations. MudPIT loading columns were prepared by briefly dipping 250 μm inner diameter (ID) undeactivated fused silica capillaries (Agilent) in 3:1 Kasil 1624 (PQ Corp) : formamide, curing overnight at 100 °C, and trimming the frit to 1 mm. The columns were then rinsed with MeOH, loaded under pressure with 2.5 cm strong cation exchange resin (SCX Luna, 5 μm diameter, 125 Å pore size, Partisphere), and loaded with another 2.5 cm reversed phase resin (C18 Aqua, 5 μm diameter, 125 Å pore size, Phenomenex). The columns were rinsed well with methanol and buffer A prior to loading the peptide digest, and further washed with buffer A. Analytical columns were prepared by pulling 100 μm ID-fused capillaries to a 5 μm ID on a P-2000 tip puller (Sutter Instrument Co.) and loaded with 15 cm of reversed phase resin, followed by methanol rinsing and equilibration in buffer A. For LC-MS/MS, each loading column was connected to the analytical column by a zero-dead-volume union, and connected to the HPLC through a tee junction that allowed connection to the 2.5 kV ESI voltage. A flow rate of 300 nL/min was maintained through a 1:1000 split flow line from an Agilent 1200 pump. MuDPIT experiments were performed where each step corresponds to 0, 10, 20, 30, 40, 50, 60, 70, 80, 90, and 100% buffer C being run for 4 min at the beginning of each gradient of buffer B. Electrospray was performed directly from the analytical column by applying the ESI voltage at a tee (150 mm ID, Upchurch Scientific) directly downstream of a 1:1000 split flow used to reduce the flow rate to 300 nL/min through the columns. Electrospray directly from the LC column was done at 2.5 kV with an inlet capillary temperature of 275 °C.

Data-dependent acquisition of MS/MS spectra were performed with the following settings: eluted peptides were scanned from 300 to 1600 m/z with resolution 30000 and the mass spectrometer in a data dependent acquisition mode. The top ten peaks for each full scan were fragmented by HCD using a normalized collision energy of 45%, a 100 ms activation time, and a resolution of 7500. Dynamic exclusion parameters were 1 repeat count, 30 ms repeat duration, 500 exclusion list size, 120 s exclusion duration, and exclusion width between 0.51 and 1.51. Protein and peptide identification and protein quantitation were done with the Integrated Proteomics Pipeline - IP2 (Integrated Proteomics Applications, Inc., San Diego, CA. http://www.integratedproteomics.com/). Tandem mass spectra were extracted from raw files using Raw Xtractor 1.9.13 and were searched against a database containing 20245 human sequences (longest entry for the IPI database for each protein) with reversed sequences using ProLuCID. Carbamidomethylation (+57.02146 Da) of cysteine and TMT tagging of N-termini and of lysine residues (+229.1629 Da) were considered as static modifications. Peptide candidates were filtered using DTASelect2 (version 2.0.27) for a false positive (decoy) peptide ratio of ~1%. Quantitation was performed using Census7, followed by deconvolution of isotopic impurity as reported in the lot analysis supplied by Thermo Fisher, and finally normalization of ratio values based on the mode. Redundant peptides were generally assigned to all proteins. The heavy to light ratio was quantified by Census (14).

SUPPORTING DATASETS

Dataset S1: GSEA results and gene sets (see attached .xlsx file).
Dataset S1A (Sheet 1). GSEA results for Tg treatment using c5bp (MSigDB), shown in Figure S1D.
Dataset S1B (Sheet 2). GSEA results for Tg treatment using c5mf (MSigDB), shown in Figure S1D.
Dataset S1C (Sheet 3). GSEA results for XBP1s activation using c5bp (MSigDB), shown in Figure S1D.
Dataset S1D (Sheet 4). GSEA results for XBP1s activation using c5mf (MSigDB), shown in Figure S1D.
Dataset S1E (Sheet 5). Full list of glycogenes in custom "lipid-linked oligosaccharide biosynthesis" and "trimming and elaboration" gene sets used for generating enrichment plots shown in Figure S8A and B.

Dataset S2. List of lectins used on the microarrays (see attached .xlsx file).
Dataset S2A (Sheet 1). List of lectins used for HEK293^{XBP1s} microarray experiments. Lectin print concentration, print sugar, and glycan epitope are indicated. Duplicate lectins obtained from different sources are noted in the last column.
Dataset S2B (Sheet 2). List of lectins used for HeLa^{XBP1s} microarray experiments. Lectin print concentration, print sugar, and glycan epitope are indicated. Duplicate lectins obtained from different sources are noted in the last column.

Dataset S3. Processed lectin microarray data (see attached .xlsx file). Data represent median normalized log2 values of sample to pooled-sample reference ratios.
Dataset S3A (Sheet 1). HEK^{XBP1s} membrane data.
Dataset S3B (Sheet 2). HeLa^{XBP1s} membrane data.
Dataset S3C (Sheet 3). HEK^{XBP1s} media data.

Dataset S4. MS analysis of the HEK^{XBP1s} secretome with XBP1s activation (see attached .xlsx file). Spectral counts, *m/z* ratios, and normalized intensities for all proteins detected by TMT-MS with or without XBP1s activation in Replicates 1–3 (Sheets 4A–4C, respectively). Processed data are presented in Sheet 4D.
Dataset S4A (Sheet 1). Full TMT-MS data for the 6 h secretome of HEK^{XBP1s} cells (Replicate 1).
Dataset S4B (Sheet 2). Full TMT-MS data for the 6 h secretome of HEK^{XBP1s} cells (Replicate 2).
Dataset S4C (Sheet 3). Full TMT-MS data for the 6 h secretome of HEK^{XBP1s} cells (Replicate 3).
Dataset S4D (Sheet 4). Fold-change and significance values for all proteins in the XBP1s secretome. Proteins that met fold-change and significance cut-offs are highlighted; significance and fold-change cut-offs were as follows: *p*-value ≤ 0.05, fold-change ≥ 1.5-fold. Proteins annotated as *N*-glycosylated (UniProtKB) are indicated along with the reported number of *N*-glycan sequons.

Dataset S5: HEK^{XBP1s} and HeLa^{XBP1s} glycogene data (see attached .xlsx file).
Dataset S5A (Sheet 1). Gene sets related to *N*-glycosylation (including glycosyltransferases, glucosidases, and sugar transporters) selected from MSigDB and used to generate Figure 5.
Dataset S5B (Sheet 2). Full list of unique genes contained in the selected gene sets listed in Dataset S5A.
Dataset S5C (Sheet 3). Fold-change and significance values for glycogenes in HEK^{XBP1s} cells with XBP1s activation used to generate Fig. 5A. Glycosylation-related genes listed in Dataset S5B were extracted from the HEK^{XBP1s} microarray data and were integrated with glycosylation PCR array data; bold-faced genes have fold-change and significance values obtained from the qPCR arrays. Significance and fold-change cut-offs were as follows: FDR or *p*-value ≤ 0.05, fold-changes ≥ 1.5-fold (XBP1s versus vehicle).
Dataset S5D (Sheet 4). Fold-change and significance values for glycogenes in HeLa^{XBP1s} cells with XBP1s activation used to generate Fig. 5C. Glycosylation-related genes listed in Dataset S5B were extracted from the HeLa^{XBP1s} RNA-Seq data and integrated with glycosylation PCR array data; bold-faced genes have fold-change and significance values obtained from the qPCR arrays. Significance and fold-change cut-offs were as follows: FDR or *p*-value ≤ 0.05, fold-changes ≥ 1.5-fold (XBP1s versus vehicle).

SUPPORTING TABLES

Table S1: GC-MS linkage analysis of partially methylated alditol acetates (PMAA) from vehicle, XBP1s-activated, and thapsigargin-treated membrane (HEK^{XBP1s} and HeLa^{XBP1s}) and secreted (HEK^{XBP1s}) glycoproteins. *N*-Linked glycans were permethylated, hydrolyzed, reduced, acetylated and analyzed by GC-MS (see Experimental Procedures).

Quantification[a]	Identification[b]	Residue	Rt (min)	HEK membrane[c]			HeLa membrane[c]			HEK secretome[c]		
				Vehicle	XBP1s	Tg	Vehicle	XBP1s	Tg	Vehicle	XBP1s	Tg
101, 102, 115, 118, 131, 162, 175	142, 187	t-Fuc	13.88	30.1	9.6	9.2	20.6	25.9	36.5	84.8	95.5	121.5
102, 118, 129, 145, 161, 162, 205	71, 87, 113, 174	t-Man	15.32	163.9	189.7	205.4	134.4	151.8	369.8	20.2	25.3	29.4
102, 118, 129, 145, 161, 162, 205	71, 87, 113, 174	t-Gal	15.59	48.6	25.3	23.4	58.7	92.5	49.1	133.1	154.9	76.9
100, 101, 129, 130, 161, 190	71, 87, 88	2-Man	16.44	276.9	297.5	335.4	321.0	300.9	460.4	190.1	222.0	308.9
130, 190, 205	87, 88, 100, 129, 145, 161, 174, 205	2-Gal	16.71	1.2	0.3	0.7	0.0	0.7	0.0	2.9	2.3	1.0
118, 143	87, 101, 129, 174, 202, 217, 234	3-Gal	16.77	29.3	6.7	4.0	26.5	25.3	11.9	56.2	36.1	61.4
102, 118, 129, 159, 162	71, 99, 143, 173, 189, 233	6-Gal	17.24	23.6	4.0	4.1	0.0	4.1	0.0	98.9	63.8	100.1
130, 190, 233	87, 88, 172, 173	2,4-Man	17.58	13.7	6.5	7.3	8.2	16.6	5.3	36.1	25.8	25.6
100, 129, 130, 189, 190	87, 88, 99, 143, 159, 173, 174	2,6-Man	17.91	30.5	11.0	9.6	16.2	26.5	9.4	105.8	71.1	36.0
118, 129, 189, 234	74, 87, 101, 160, 174, 202, 245	3,6-Man	18.15	98.6	99.6	99.2	100.0	100.0	100.0	95.3	97.7	96.3
118, 129, 189, 234	74, 87, 101, 160, 174, 202	3,6-Gal	18.32	n.d.[d]	n.d.	n.d.	11.9	16.4	6.7	n.d.	n.d.	n.d.
118, 139	87, 97, 129, 160, 202	3,4,6-Man	18.56	1.4	0.4	0.8	n.d.	n.d.	n.d.	4.7	2.3	3.7
117, 129, 143, 145, 159, 203, 205	75, 187, 217	t-GlcNAc	18.98	2.4	1.8	4.2	1.9	2.1	0.0	4.8	2.7	1.3
117, 159, 233	75, 99, 143, 171, 203	4-GlcNAc	19.83	163.1	56.0	70.1	66.0	206.7	35.3	415.7	108.7	89.1
117, 142, 159	75, 99, 171, 231, 244	3,4-GlcNAc	20.62	1.5	0.9	0.8	1.2	2.8	10.0	5.8	5.2	2.2
117, 159	75, 99, 124, 127, 142, 143, 201, 245	4,6-GlcNAc	21.05	6.6	1.8	3.7	5.4	10.6	3.1	30.3	11.9	10.9

[a] Electron impact fragment ions used for quantification of the PMAA residues. For relative abundance, in order to minimize interference from the baseline and/or contamination, all fragment ions greater than 100 (>100) were used for the extracted ion current (XIC) chromatogram, as indicated above.

[b] Electron impact fragment ions used for identification of the PMAA residues, in addition to the ions used for quantification.

[c] Relative abundances were obtained by normalizing the integrated area peak of the extracted ion current (XIC) chromatogram of a specific residue to the summed integrated areas of the XICs of 3,6-linked mannose and 3,4,6-linked mannose.

[d] *n.d.* = not detected.

Table S2: Summary of observed changes to the HEK^{XBP1s} and HeLa^{XBP1s} *N*-glycomes with XBP1s activation.

Observed Change with XBP1s	HEK^{XBP1s} Membrane	HEK^{XBP1s} Secretome	HeLa^{XBP1s} Membrane
Increased high-mannose		✓	✓
Decreased sialylation	✓	✓	
Decreased bisecting GlcNAc	✓	✓	
Increased core fucosylation			✓
Increased tetra-antennary glycans			✓

Table S3: Summary of observed changes to the HEK^{XBP1s} and HeLa^{XBP1s} *N*-glycomes with global UPR activation by treatment with Tg.

Observed Change with Tg	HEK^{XBP1s} Membrane	HEK^{XBP1s} Secretome	HeLa^{XBP1s} Membrane
Increased high-mannose			✓
Decreased sialylation	✓	✓	
Decreased bisecting GlcNAc	✓	✓	
Increased core fucosylation			
Decreased branching		✓	✓
Increased core 1/3 *O*-glycans	✓		

SUPPORTING FIGURE LEGENDS

Figure S1: Characterization of HEK^{XBP1s} and HeLa^{XBP1s} cell lines.
Transcript levels of genes regulated by the IRE1-XBP1s arm (*ERDJ4* and *SEC24D*) or the PERK-ATF4 arm (*CHOP* and *GADD34*) of the UPR were measured in HEK^{XBP1s} cells (A) and HeLa^{XBP1s} cells (B) by qRT-PCR. (C) RNA-Seq highlights distinctive effects of stress-mediated global UPR activation versus stress-independent XBP1s activation. Hierarchical clustering of differentially expressed protein-coding genes. HeLa^{XBP1s} cells were plated at a density of 6 × 10^5 cells per well in 6-well plates and allowed to adhere overnight. Cells were then treated with dox (1 μg/mL, 48 h), DMSO (0.1%, 24 h), or thapsigargin (Tg; 750 nM, 24 h), total RNA was extracted with the Qiagen RNeasy Plus Mini Kit, and samples were loaded on a HiSeq cartridge. Supervised hierarchical clustering was performed using Ward's method implemented in Spotfire 7.6.1 with row-centered log2 FPKM data for genes differentially expressed in at least one of the following comparisons: Tg vs vehicle, XBP1s vs vehicle, or XBP1s vs Tg. For the hierarchical clustering, differentially expressed genes were defined as those having absolute log2 fold-change > 1 and FDR adjusted *p*-values < 0.05. (D) Selected GSEA enrichment plots for XBP1s versus vehicle and Tg versus vehicle showing distinct effects of XBP1s-activation versus global UPR activation with the ER stressor Tg.

Figure S2: Freestyle and complete DMEM media Western blot
Western blot of conditioned media from HEK^{XBP1s} cells cultured in complete DMEM or Freestyle media, shown at both low and high exposure. HEK^{XBP1s} cells were plated at a density of 6 × 10^5 cells per well on poly-D-lysine coated 6-well plates and allowed to adhere overnight. Cells were then treated with or without dox (1 μg/mL, 24 h), after which plates were washed three times with PBS (containing Ca^{2+} and Mg^{2+}) prior to treatment with either full DMEM (+10% FBS, L-glutamine) or Freestyle media, with or without 1 μg/mL dox. Conditioned media was collected for 48 h, spun at 1.5k RPM at 4 °C for 5 min to pellet cell debris, and then run on 4/8% SDS-PAGE polyacrylamide gels. Grp78 signal was detectable in Freestyle media samples, but only upon XBP1s activation.

Figure S3: Analysis of the HEK^{XBP1s} membrane glycoproteome
(A) Lectin microarray analysis of membrane proteomes isolated from HEK^{XBP1s} cells showed decreased sialylation and a loss of bisecting GlcNAc upon XBP1s activation (left panel). Tg treatment (right panel) also showed decreases in sialylation and bisecting GlcNAc, along with an increase in core 1/3 *O*-glycans. Spot colors correspond to lectin sugar specificity, as indicated; the dotted line represents a significance cutoff of *p*-value ≤ 0.05 across three biological replicates. (B) MALDI-TOF MS spectra of high mass *N*-glycans. Red, yellow and green peaks correspond to tetra-antennary *N*-glycans with 2, 3 and 4 additional LacNAc repeats, respectively, with various levels of sialylation. Yellow and green shaded areas, manually inserted, highlight the shift towards fewer NeuAc residues. Structures outside a bracket have not been unequivocally defined, and "M," "m," and "vm," designations indicate major, minor and very minor abundances, respectively. Putative structures were assigned based on glycan composition, tandem mass spectrometry data, and knowledge of biosynthetic pathways. (C) Zoomed-in MALDI-TOF MS spectra indicating bi-antennary N-glycans (red peaks) with varying levels of sialylation. Putative structures were assigned based on glycan composition, tandem mass spectrometry data, and knowledge of biosynthetic pathways. (D) MALDI-TOF/TOF MS/MS spectra (selected from corresponding panels in Fig. S3B) for vehicle, XBP1s-activated, and Tg-treated HEK^{XBP1s} membrane proteomes. Spectra depict fragments of the $[M+Na]^+$ molecular ion found at *m/z* 5124. Structures above each horizontal dashed arrow indicate loss of the designated *N*-glycan sequence from the molecular ion; vertical dashed lines indicate the corresponding fragment ion peak. All molecular and fragment ions are $[M+Na]^+$. Cartoon structures were drawn according to the Consortium for Functional Glycomics (http://www.functionalglycomics.org) guidelines. For the molecular ion at *m/z* 5124, note the fragment ions at *m/z* 4300, 3850, 3401 and 2952 that correspond to loss of sialylated-LacNAc, sialylated-$LacNAc_2$, sialylated-$LacNAc_3$ and sialylated-$LacNAc_4$ respectively. The presence of such fragment ions suggests the existence of structural isomers corresponding mainly to tetra-antennary (and to a lesser extent tri-antennary) *N*-glycans. The relative abundance of these fragment ions did not shift between vehicle-treated, XBP1s-activated and Tg-treated HEK^{XBP1s} cells, further suggesting that the ratio of structural isomers remained relatively constant.

Figure S4: Differences in baseline HEK^{XBP1s} and HeLa^{XBP1s} membrane glycoproteomes
Heat map of lectin microarray data generated from isolated HEK^{XBP1s} and HeLa^{XBP1s} membrane glycoproteomes under vehicle-treated conditions. Samples were run on the same lectin microarray slide. Color intensity represents normalized log2 ratio data relative to a pooled (in this case, multi-cell line) sample reference. Each column represents one biological replicate of the indicated sample.

Figure S5: Analysis of the HeLa^{XBP1s} membrane N-glycoproteome
(A) MALDI-TOF MS spectra of high mass *N*-glycans and (B) MALDI-TOF/TOF MS/MS spectra (selected from corresponding panels in Fig. S5A) for vehicle, XBP1s-activated, and Tg-treated HeLa^{XBP1s} membrane proteomes. MALDI-TOF/TOF MS/MS spectra depict fragments of the $[M+Na]^+$ molecular ion found at *m/z* 5300. (C) Lectin microarray analysis of membrane proteomes isolated from HeLa^{XBP1s} cells showed an increase in high-mannose *N*-glycans upon XBP1s activation (left panel), as well as increases in core fucosylation and tetra-antennary *N*-glycans (β1,6-GlcNAc). Tg activation (right panel) showed a similar gain of high-mannose *N*-glycans, but not increased β1,6-GlcNAc branching. Spot colors correspond to lectin sugar specificity; the dotted line represents a significance cutoff of *p*-value ≤ 0.05 across three biological replicates.

Figure S6: Lectin flow cytometry confirms that XBP1s activation increases high-mannose *N*-glycans on HeLa^{XBP1s} cells
(A) Lectin flow cytometry on live HeLa^{XBP1s} cells confirmed the increase in levels of high-mannose *N*-glycans on the cell surface (left panel, histogram; middle panel, quantification). Inhibitory sugar controls (right panel) were performed with methyl-mannose. Cell viability analyzed by CellTiter-Glo (B) or resazurin assay (C) was not significantly affected by treatment with dox (1 μg/mL, 72 h) or 1-deoxymannojirimycin (1-DMM, Sigma-Aldrich; 80 μg/mL, 24 h). 1×10^4 HeLa^{XBP1s} cells were seeded for each well 24 h prior to measurements. Error bars represent SEM from four replicates. (D) To verify that HHL recognized high-mannose glycans, HeLa^{XBP1s} cells were treated with 80 μg/mL of 1-DMM for 12 h to inhibit mannosidase-I and thus increase high-mannose N-glycan levels prior to analysis.

Figure S7: Analysis of the HEK^{XBP1s} secreted glycoproteome
Lectin microarray analysis of the HEK^{XBP1s} secretome showed a decrease in bisecting GlcNAc and an increase in early processed *N*-glycans upon XBP1s activation (left panel). Tg treatment (right panel) showed a decrease in multi-antennary *N*-glycans with no gain in high-mannose structures. Spot colors correspond to lectin sugar specificity; the dotted line represents a significance cutoff of *p*-value ≤ 0.05 across three biological replicates.

Figure S8: XBP1s impacts expression of genes involved in lipid-linked oligosaccharide biosynthesis
(A) GSEA enrichment plots for HEK^{XBP1s} microarray data upon XBP1s activation using the custom gene sets listed in Dataset S1E. Standard GSEA was run using signal-to-noise ratio as a ranking metric. (B) Enrichment plots for HeLa^{XBP1s} RNA-Seq data upon XBP1s activation using the custom gene sets listed in Dataset S1E. Standard GSEA was run using signal-to-noise ratio as a ranking metric.

Figure S9: XBP1s impacts expression of genes involved in nucleotide sugar donor biosynthesis
Simplified biosynthetic pathway of nucleotide sugars depicting the enzymes/transporters that are significantly upregulated upon XBP1s activation in HeLa^{XBP1s} cells. Transcripts shown in green (all with significant expression changes based on FDR or *p*-value ≤ 0.05) encode enzymes or transporters with a fold-change ≥ 1.5, while genes in black encode enzymes with fold-change between 1.0–1.5-fold. Note that *GNPDA1*, which together with *GNPDA2* catalyzes the reverse reaction of *GFPT1*, was significantly decreased (0.79-fold) in HeLa^{XBP1s} cells (Dataset S5D). Biosynthetic pathway adapted from Freeze et al. (15) and the KEGG database (*Homo sapiens* nucleotide sugar metabolism, http://www.kegg.jp).

FIGURE S1

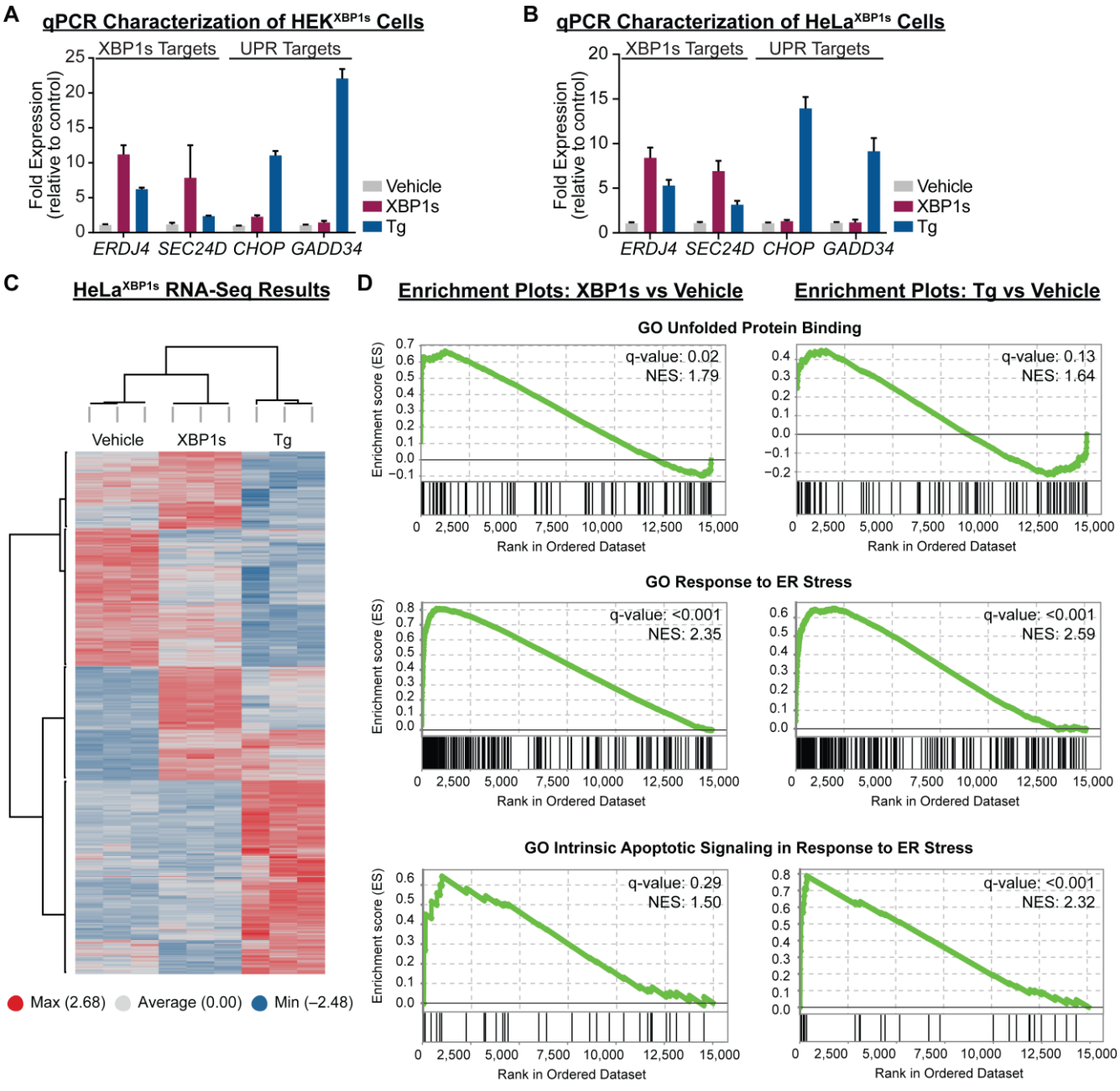
A
qPCR Characterization of HEK^XBP1s Cells
XBP1s Targets
UPR Targets
Fold Expression (relative to control)
Vehicle
XBP1s
Tg
ERDJ4 SEC24D CHOP GADD34
B
qPCR Characterization of HeLa^XBP1s Cells
C
HeLa^XBP1s RNA-Seq Results
Vehicle
XBP1s
Tg
Max (2.68) Average (0.00) Min (–2.48)
D
Enrichment Plots: XBP1s vs Vehicle
Enrichment Plots: Tg vs Vehicle
GO Unfolded Protein Binding
q-value: 0.02
NES: 1.79
q-value: 0.13
NES: 1.64
GO Response to ER Stress
q-value: <0.001
NES: 2.35
q-value: <0.001
NES: 2.59
GO Intrinsic Apoptotic Signaling in Response to ER Stress
q-value: 0.29
NES: 1.50
q-value: <0.001
NES: 2.32
Enrichment score (ES)
Rank in Ordered Dataset

FIGURE S2

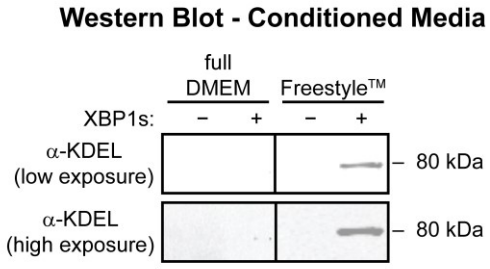
Western Blot - Conditioned Media
full
DMEM
Freestyle™
XBP1s:
–
+
–
+
α-KDEL
(low exposure)
80 kDa
α-KDEL
(high exposure)
80 kDa

FIGURE S3

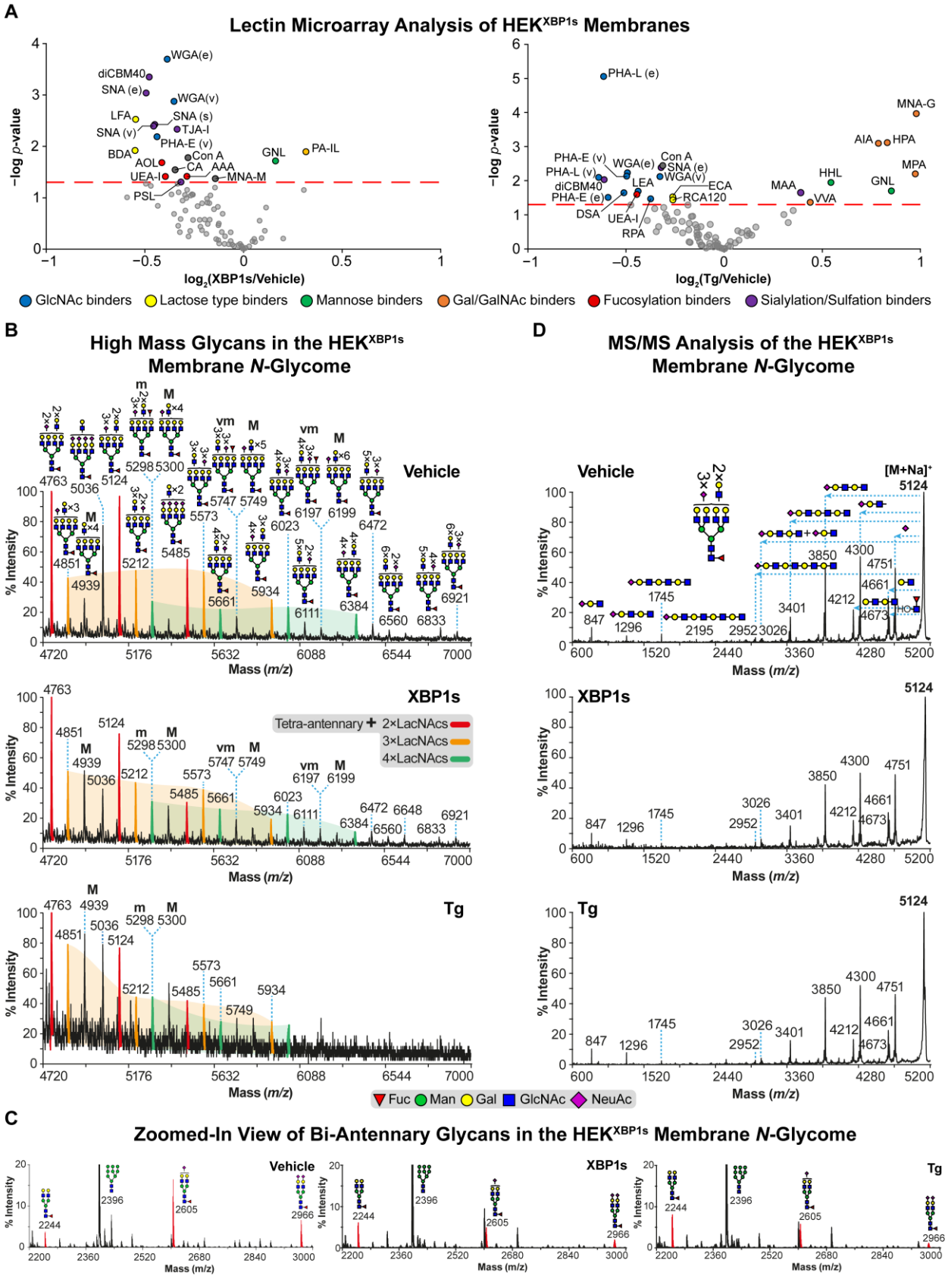
A
Lectin Microarray Analysis of HEK^XBP1s Membranes
−log p-value
log2(XBP1s/Vehicle)
log2(Tg/Vehicle)
WGA(e)
diCBM40
SNA (e)
WGA(v)
LFA
SNA (s)
SNA (v)
TJA-I
PHA-E (v)
BDA
Con A
GNL
PA-IL
AOL
CA
AAA
UEA-I
MNA-M
PSL
PHA-L (e)
MNA-G
AIA
HPA
PHA-E (v)
WGA(e)
Con A
PHA-L (v)
SNA (e)
MPA
HHL
diCBM40
LEA
WGA(v)
ECA
GNL
MAA
PHA-E (e)
RCA120
VVA
DSA
UEA-I
RPA
GlcNAc binders
Lactose type binders
Mannose binders
Gal/GalNAc binders
Fucosylation binders
Sialylation/Sulfation binders
B
High Mass Glycans in the HEK^XBP1s Membrane N-Glycome
Vehicle
XBP1s
Tg
% Intensity
Mass (m/z)
Tetra-antennary + 2×LacNAcs
3×LacNAcs
4×LacNAcs
D
MS/MS Analysis of the HEK^XBP1s Membrane N-Glycome
Vehicle
XBP1s
Tg
[M+Na]+
5124
% Intensity
Mass (m/z)
Fuc
Man
Gal
GlcNAc
NeuAc
C
Zoomed-In View of Bi-Antennary Glycans in the HEK^XBP1s Membrane N-Glycome
Vehicle
XBP1s
Tg
% Intensity
Mass (m/z)

FIGURE S4

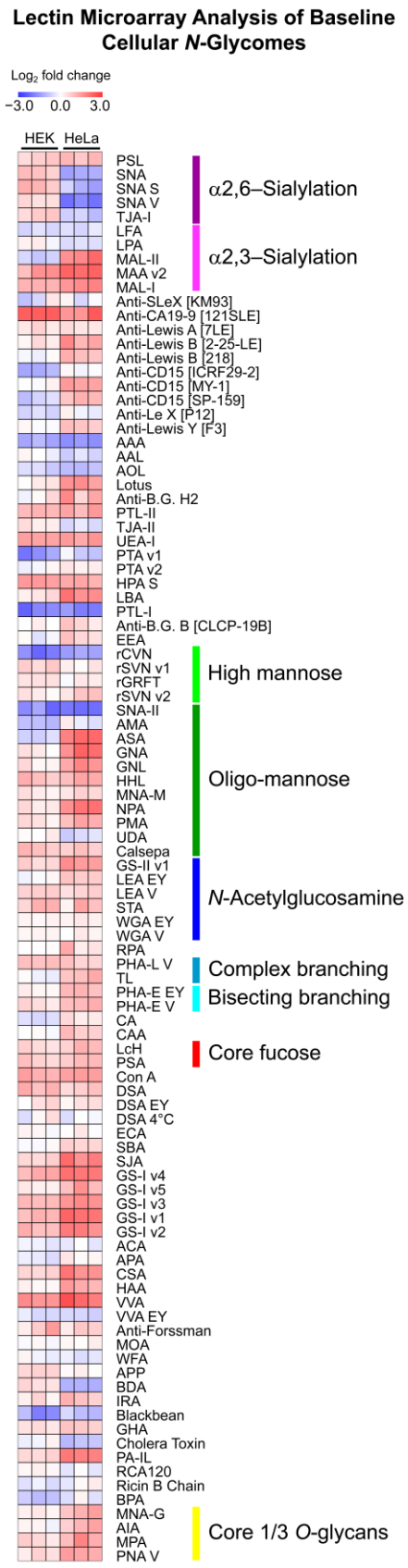
Lectin Microarray Analysis of Baseline Cellular N-Glycomes
Log2 fold change
−3.0 0.0 3.0
HEK HeLa
PSL
SNA
SNA S
SNA V
TJA-I
LFA
LPA
MAL-II
MAA v2
MAL-I
Anti-SLeX [KM93]
Anti-CA19-9 [121SLE]
Anti-Lewis A [7LE]
Anti-Lewis B [2-25-LE]
Anti-Lewis B [218]
Anti-CD15 [ICRF29-2]
Anti-CD15 [MY-1]
Anti-CD15 [SP-159]
Anti-Le X [P12]
Anti-Lewis Y [F3]
AAA
AAL
AOL
Lotus
Anti-B.G. H2
PTL-II
TJA-II
UEA-I
PTA v1
PTA v2
HPA S
LBA
PTL-I
Anti-B.G. B [CLCP-19B]
EEA
rCVN
rSVN v1
rGRFT
rSVN v2
SNA-II
AMA
ASA
GNA
GNL
HHL
MNA-M
NPA
PMA
UDA
Calsepa
GS-II v1
LEA EY
LEA V
STA
WGA EY
WGA V
RPA
PHA-L V
TL
PHA-E EY
PHA-E V
CA
CAA
LcH
PSA
Con A
DSA
DSA EY
DSA 4°C
ECA
SBA
SJA
GS-I v4
GS-I v5
GS-I v3
GS-I v1
GS-I v2
ACA
APA
CSA
HAA
VVA
VVA EY
Anti-Forssman
MOA
WFA
APP
BDA
IRA
Blackbean
GHA
Cholera Toxin
PA-IL
RCA120
Ricin B Chain
BPA
MNA-G
AIA
MPA
PNA V
α2,6–Sialylation
α2,3–Sialylation
High mannose
Oligo-mannose
N-Acetylglucosamine
Complex branching
Bisecting branching
Core fucose
Core 1/3 O-glycans

FIGURE S5

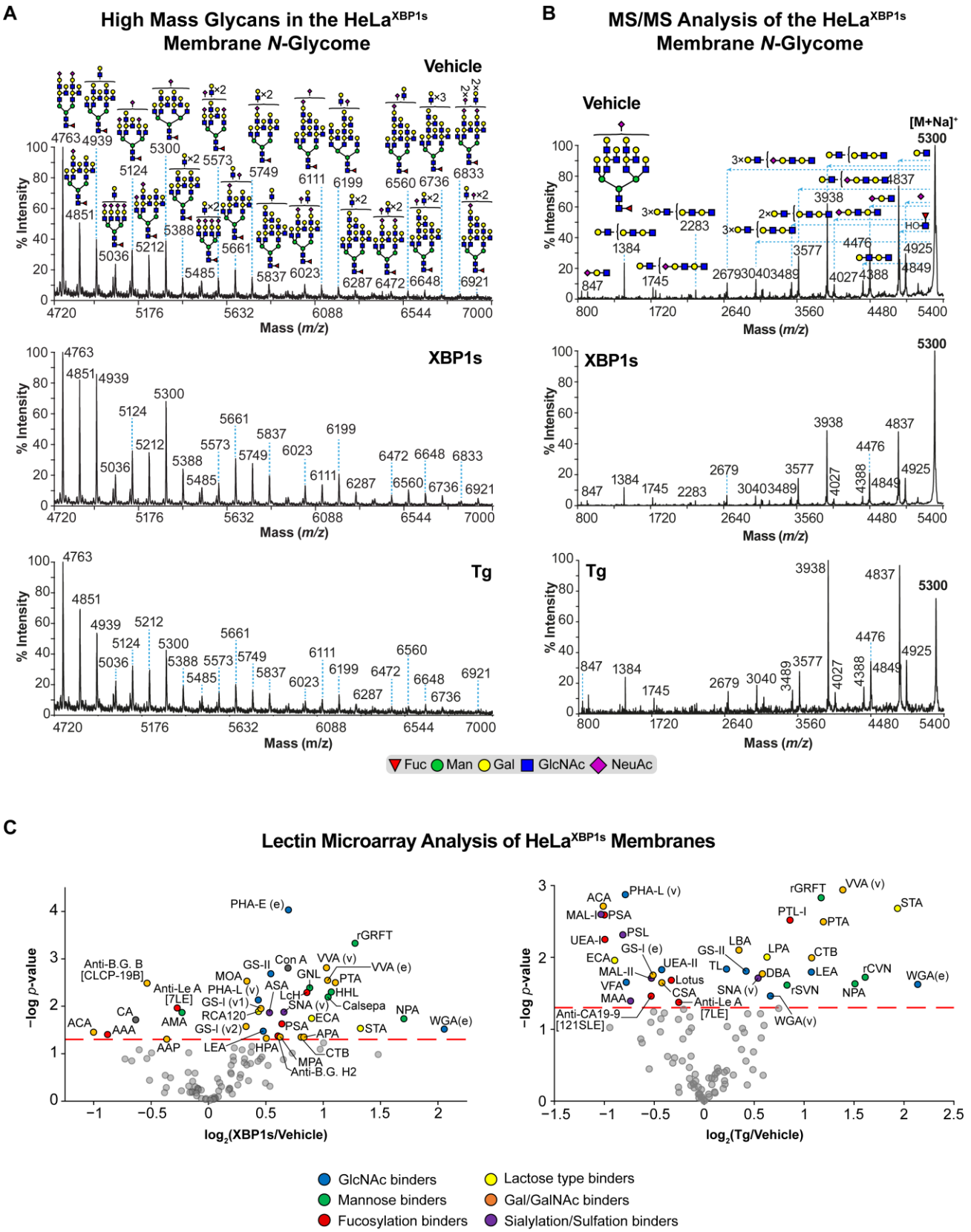
A
High Mass Glycans in the HeLa XBP1s Membrane N-Glycome
Vehicle
XBP1s
Tg
% Intensity
Mass (m/z)
B
MS/MS Analysis of the HeLa XBP1s Membrane N-Glycome
Vehicle
XBP1s
Tg
[M+Na]+
Fuc Man Gal GlcNAc NeuAc
C
Lectin Microarray Analysis of HeLa XBP1s Membranes
−log p-value
log2(XBP1s/Vehicle)
log2(Tg/Vehicle)
GlcNAc binders
Mannose binders
Fucosylation binders
Lactose type binders
Gal/GalNAc binders
Sialylation/Sulfation binders

FIGURE S6

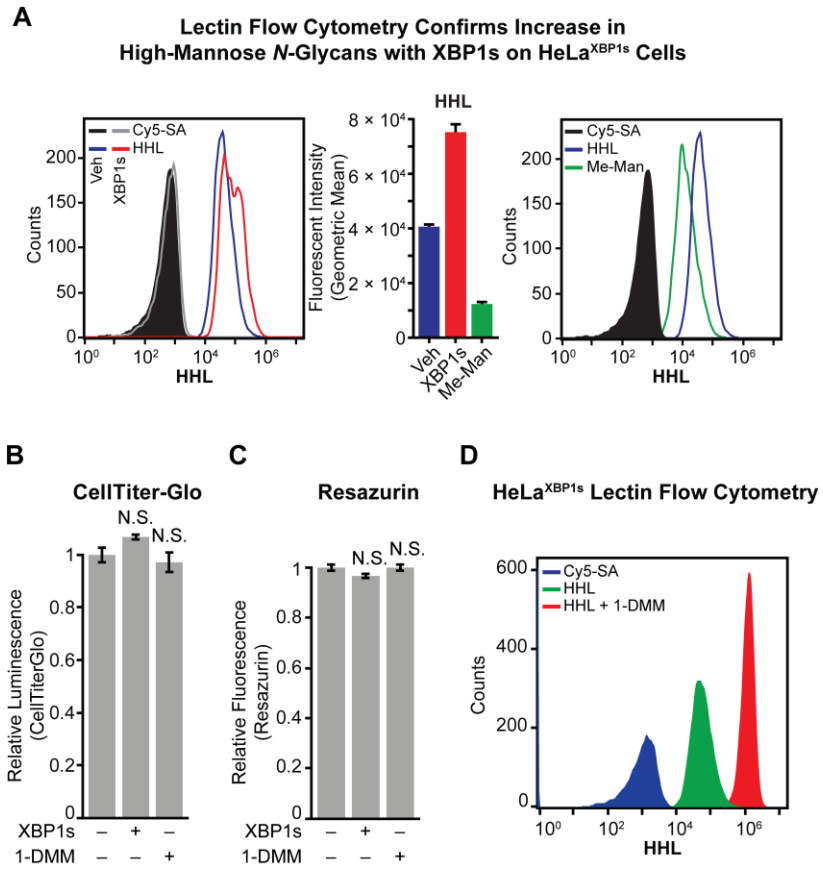
A
Lectin Flow Cytometry Confirms Increase in
High-Mannose N-Glycans with XBP1s on HeLa^XBP1s Cells
Cy5-SA
HHL
Veh
XBP1s
Counts
HHL
Fluorescent Intensity (Geometric Mean)
Me-Man
B
CellTiter-Glo
Relative Luminescence (CellTiterGlo)
N.S.
XBP1s
1-DMM
C
Resazurin
Relative Fluorescence (Resazurin)
D
HeLa^XBP1s Lectin Flow Cytometry
HHL + 1-DMM

FIGURE S7

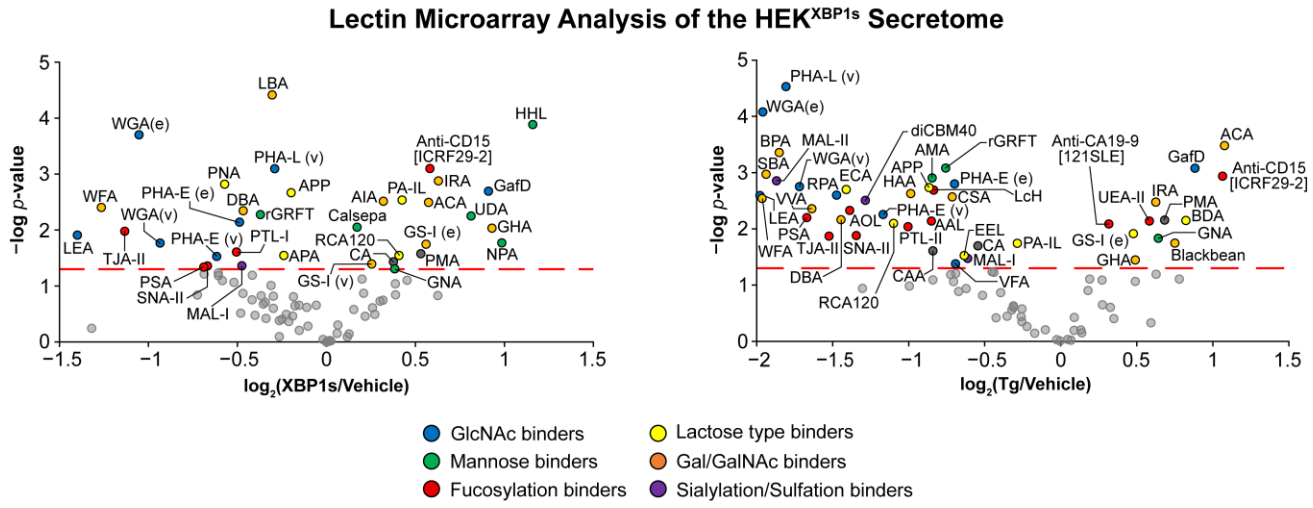
Lectin Microarray Analysis of the HEK^XBP1s Secretome
−log p-value
log2(XBP1s/Vehicle)
LBA
WGA(e)
HHL
Anti-CD15 [ICRF29-2]
PHA-L (v)
PNA
APP
IRA
GafD
WFA
PHA-E (e)
DBA
PA-IL
AIA
ACA
UDA
WGA(v)
rGRFT
Calsepa
GHA
GS-I (e)
LEA
PHA-E (v)
PTL-I
RCA120
TJA-II
APA
CA
PMA
NPA
PSA
GS-I (v)
GNA
SNA-II
MAL-I
log2(Tg/Vehicle)
PHA-L (v)
WGA(e)
diCBM40
rGRFT
Anti-CA19-9 [121SLE]
ACA
BPA
MAL-II
AMA
GafD
SBA
WGA(v)
ECA
APP
Anti-CD15 [ICRF29-2]
RPA
HAA
PHA-E (e)
VVA
CSA
LcH
UEA-II
IRA
LEA
PHA-E (v)
PMA
AOL
AAL
BDA
PSA
EEL
GNA
PTL-II
WFA
TJA-II
SNA-II
CA
PA-IL
GS-I (e)
Blackbean
MAL-I
GHA
DBA
CAA
VFA
RCA120
GlcNAc binders
Mannose binders
Fucosylation binders
Lactose type binders
Gal/GalNAc binders
Sialylation/Sulfation binders

FIGURE S8

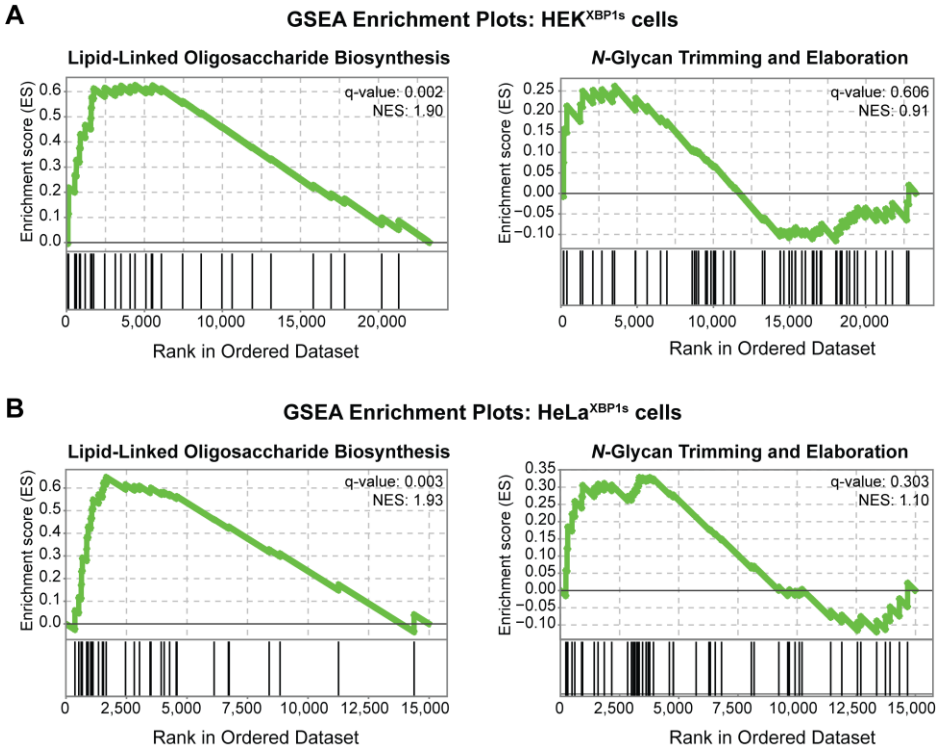
A
GSEA Enrichment Plots: HEK^{XBP1s} cells
Lipid-Linked Oligosaccharide Biosynthesis
q-value: 0.002
NES: 1.90
Enrichment score (ES)
Rank in Ordered Dataset
N-Glycan Trimming and Elaboration
q-value: 0.606
NES: 0.91
Enrichment score (ES)
Rank in Ordered Dataset
B
GSEA Enrichment Plots: HeLa^{XBP1s} cells
Lipid-Linked Oligosaccharide Biosynthesis
q-value: 0.003
NES: 1.93
Enrichment score (ES)
Rank in Ordered Dataset
N-Glycan Trimming and Elaboration
q-value: 0.303
NES: 1.10
Enrichment score (ES)
Rank in Ordered Dataset

FIGURE S9

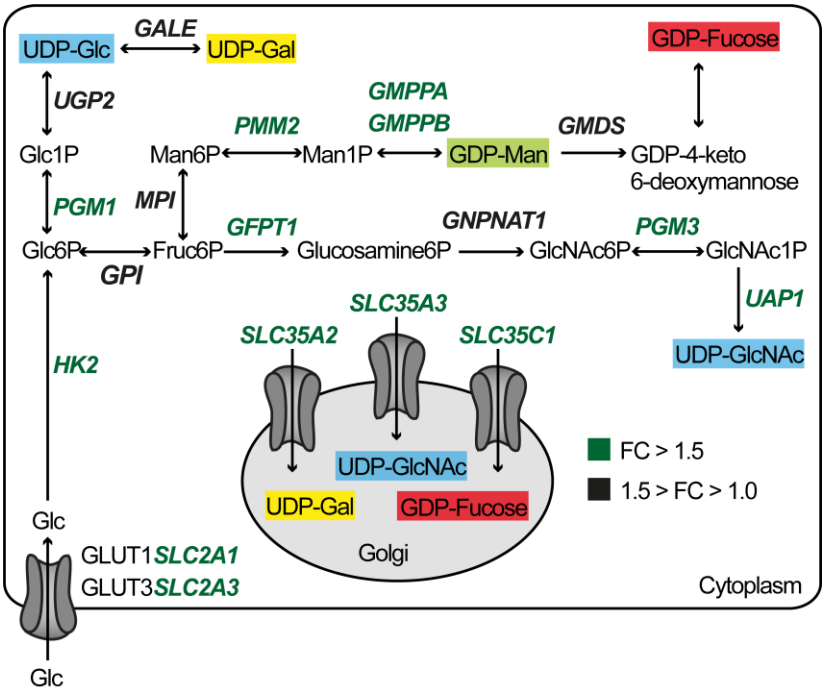
GALE
UDP-Glc
UDP-Gal
GDP-Fucose
UGP2
GMPPA
GMPPB
PMM2
GMDS
Glc1P
Man6P
Man1P
GDP-Man
GDP-4-keto
6-deoxymannose
PGM1
MPI
GFPT1
GNPNAT1
PGM3
Glc6P
Fruc6P
Glucosamine6P
GlcNAc6P
GlcNAc1P
GPI
UAP1
SLC35A3
SLC35A2
SLC35C1
HK2
UDP-GlcNAc
FC > 1.5
1.5 > FC > 1.0
UDP-GlcNAc
UDP-Gal
GDP-Fucose
Golgi
Glc
GLUT1 SLC2A1
GLUT3 SLC2A3
Cytoplasm
Glc

SUPPORTING REFERENCES

1. Dewal MB, et al. (2015) XBP1s links the unfolded protein response to the molecular architecture of mature N-glycans. *Chem Biol* **22**:1301-1312.
2. Pilobello KT, et al. (2013) Advances in lectin microarray technology: Optimized protocols for piezoelectric print conditions. *Curr Protoc Chem Biol* **5**:1-23.
3. Jang-Lee J, et al. (2006) Glycomic profiling of cells and tissues by mass spectrometry: Fingerprinting and sequencing methodologies. *Methods Enzymol* **415**:59-86.
4. Chen C, et al. (2012) Glycoengineering approach to half-life extension of recombinant biotherapeutics. *Bioconjug Chem* **23**:1524-1533.
5. Ceroni A, et al. (2008) GlycoWorkbench: A tool for the computer-assisted annotation of mass spectra of glycans. *J Proteome Res* **7**:1650-1659.
6. Monk CR, et al. (2006) Letter to the Glyco-Forum: Preparation of CD25+ and CD25− CD4+ T cells for glycomic analysis—a cautionary tale of serum glycoprotein sequestration. *Glycobiology* **16**:11G-13G.
7. Chen Q, et al. (2015) Global N-linked glycosylation is not significantly impaired in myoblasts in congenital myasthenic syndromes caused by defective glutamine-fructose-6-phosphate transaminase 1 (GFPT1). *Biomolecules* **5**:2758-2781.
8. Rillahan CD, et al. (2012) Global metabolic inhibitors of sialyl- and fucosyltransferases remodel the glycome. *Nat Chem Biol* **8**:661-668.
9. Shoulders MD, et al. (2013) Stress-independent activation of XBP1s and/or ATF6 reveals three functionally diverse ER proteostasis environments. *Cell Rep* **3**:1279-1292.
10. Langmead B, et al. (2009) Ultrafast and memory-efficient alignment of short DNA sequences to the human genome. *Genome Biol* **10**:R25.
11. Li B, et al. (2011) RSEM: Accurate transcript quantification from RNA-seq data with or without a reference genome. *BMC Bioinform* **12**:323.
12. Love MI, et al. (2014) Moderated estimation of fold change and dispersion for RNA-seq data with DESeq2. *Genome Biol* **15**:550.
13. Subramanian A, et al. (2005) Gene set enrichment analysis: A knowledge-based approach for interpreting genome-wide expression profiles. *Proc Natl Acad Sci U S A* **102**:15545-15550.
14. Park SK, et al. (2008) A quantitative analysis software tool for mass spectrometry-based proteomics. *Nat Methods* **5**:319-322.
15. Freeze HH, et al. (2017) Glycosylation precursors. *Essentials of Glycobiology* ed Varki A CR, Esko JD, et al. (Cold Spring Harbor Laboratory Press, Cold Spring Harbor (NY)), 3 Ed.